CHAPTER 7

Magnetic Spin Dynamics in Magnetite-Silver Core-Shell Nanoparticles

7.1 Introduction

Apart from structural, optical and magnetic properties as discussed in chapter 4, 5 and 6, the application of these materials in biomedical field requires a lot of investigation about its magnetic spin dynamics. The complexity in the core-shell structure at nanoscale level affects the dynamical response of the system which needs to be explored. For a magnetic nanoparticle to be employed as MR contrast enhancement agent, the magnetic spin relaxation of the system needs to be studied since it crucially affects the MR signals.

The different effective anisotropies of two layers can modify the relaxation mechanism of magnetic moments. From the magnetic properties aspect (as discussed in Chapter 6), a single nanoparticle consists of three layers: a magnetically ordered core, an intermediate layer with disordered spins and a non-magnetic shell. A sufficient quantity of literature that describes the relaxation studies by ac susceptibility measurements and time decay of thermoremanent magnetization (TRM) can be found for magnetic systems

with same magnetic properties throughout [87,201-202]. The study of magnetic spin behavior and their interactions at core-shell interface is still very limited which needs to be explored. This chapter includes the relaxation studies of nanoparticle system exhibiting different kinds of magnetic behavior in a single nanostructure.

The spin dynamics of uncoated magnetite nanoparticles with average particle size ~6 nm, coated with ~2 nm and ~ 4 nm thick silver shell have been studied using different magnetization measurements protocol. The analysis of ac susceptibility measurements and thermoremanent magnetization studies are carried out to probe the effect of the disordered spin layer on relaxation of magnetization in both uncoated and silver coated magnetite nanoparticles.

7.2 Evidence of Spin-Glass Behavior in Coated Nanoparticles

The temperature dependence measurement of ac magnetization for several frequencies ranging from 9 Hz to 941 Hz is carried out. The sample is cooled down to 2 K from room temperature in absence of magnetic field. A probing alternating magnetic field of magnitude 3 Oe is applied in order to measure the ac susceptibility and temperature is raised to 300 K in fixed short steps. Figure 7.1 shows the real part of ac susceptibility, χ' of the uncoated magnetite, ~2 nm and ~4 nm thick silver shell coated Fe_3O_4. The curves at each frequency show a maximum at certain temperature. With an increase in frequency, the value of χ' decreases while the peak temperature increases for both uncoated and coated nanoparticle systems. This behavior is in accordance with that of bare magnetite nanoparticles of size 5 nm as reported in the literature [84]. This χ_{ac} dependence on temperature is a characteristic property of both superparamagnetic and spin-glass behavior. The cusp observed in ac susceptibility for canonical spin glasses are not observable here as very low magnitude dc magnetic fields could round the cusp up.

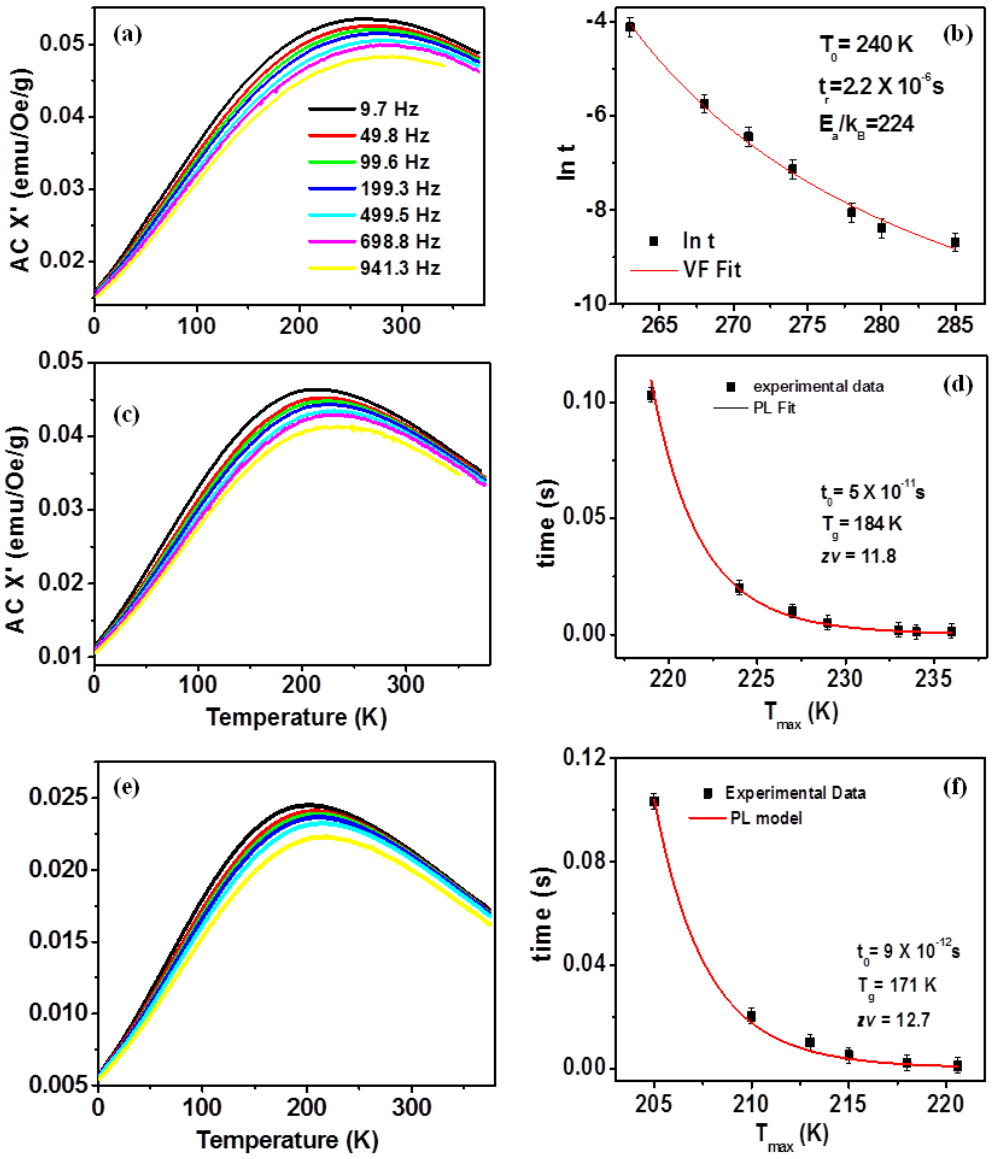

Figure 7.1. AC magnetic susceptibility curves in temperature range 2 K to 300 K at different frequencies for (a) magnetite nanoparticles, (c) ~2 nm thick silver shell and (e) ~4 nm thick silver shell. The curves (b), (d) and (f) shows Vogel-Fulcher law and power law fit of the experimental data of time vs T_{max} for (a) and (c), respectively.

In order to further verify the spin-glass behavior, a quantitative relative peak shift with frequency is calculated as [105]:

$$\emptyset = \frac{\Delta T_{max}}{T_{max}(f)\Delta \log(f)} \tag{7.1}$$

This quantity Ø is of the order 0.3 for superparamagnets, whereas it lies between 0.005-0.010 for metallic spin glasses and in the range 0.06-0.08 for insulating spin glass materials [106]. In case of magnetite nanoparticles, the value of Ø is obtained to be 0.13, which indicates the presence of weakly interacting superparamagnetic behavior in the synthesized material. This value of Ø is found to be 0.0294 and 0.038 for ~2 nm and ~4 nm thick silver shell coated Fe_3O_4, nanoparticles, respectively. In current investigation, it is evident that the value *Ø* indicates the spin glass behavior of coated iron oxide nanoparticles. The spin glass hypothesis of the sample leads to basically two distinct explanations of spin- glass freezing. The first possible interpretation indicates existence of a finite temperature for equilibrium phase transition (canonical spin glasses). The second one emphasizes on the occurrence of magnetic clusters where freezing no longer remains an equilibrium phenomenon and hence is a non- equilibrium one [203].

The dynamics of isolated spin clusters or superparamagnets are described using Néel-Arrhenius law [204]:

$$\tau = \tau_0 exp\left(\frac{-E_a}{k_B T_f}\right); \quad (7.2)$$

where τ is the time of particle magnetization flips in between two minimum energy states and τ_0 is the attempt time which generally occurs ranges between 10^{-13} to 10^{-15}s for superparamagnetic nanoparticles. E_a is the energy barrier that separates two low energy states, which corresponds to the anti- parallel or parallel alignment with easy magnetization axis of ferro- or ferrimagnetic alignment. The linear fit corresponding to the equation 7.2 for plot of $\frac{1}{T}$ with $\ln\tau$ for χ' in case of bare magnetite nanoparticles gives $\tau_0$value of the order 10^{-30} s and $\frac{E_a}{k_B} = 17585$ K. In case of ~2 nm thick silver coated magnetite nanoparticles, the fitting parameters are found to be $\tau_0 \sim 10^{-36}$ s and

$\frac{E_a}{k_B} = 18456$ K. In case of 4 nm thick silver coated magnetite nanoparticles, these parameters are found to be $\tau_0 \sim 10^{-36}$ s and $\frac{E_a}{k_B} = 18750$ K. In all the three cases, the fitting parameter values are quite unphysical. This analysis demonstrates that sample under investigation do not follows Néel-Arrhenius formalism. To gain some further physical insights of the magnetic system, the particle- particle interactions are taken into account. For weakly interacting magnetic clusters, a phenomenological Vogel- Fulcher law has been proposed with an additional term T_0 to take care of the inter- cluster interactions [107] :

$$\tau = \tau_0 exp\left(\frac{-E_a}{k_B(T_f - T_0)}\right) \quad (7.3)$$

The equation implies a linear dependence of peak temperature (more correctly referred as blocking temperature in this context) with ln τ. From the best linear fit of our data, the obtained values for bare magnetite nanoparticle systems are $\tau_0 \approx 2.2 \times 10^{-6} s$, T_0=240 K and $\frac{E_a}{k_B} = 224$ and for ~2 nm thick silver coated magnetite nanoparticles, the values of parameters are found to be $\tau_0 \approx 1 \times 10^{-16} s$, T_0=139.3 K and $\frac{E_a}{k_B} = 3311$. These values are found to be $\tau_0 \approx 1 \times 10^{-12} s$, T_0=123 K and $\frac{E_a}{k_B} = 941$ for ~4 nm thick silver shell coated magnetite nanoparticles. The fitting parameter values observed for uncoated magnetite nanoparticles lie in the range expected for non-interacting superparamagnetic systems (figure 7.1(b)) which agrees well with the magnetic behavior interpreted using the value of Ø. In case of silver coated magnetite nanoparticles, these values do not match with the range reported for superparamagnetic system. The spin-glass systems usually give these types of unreasonable numbers [110]. The third approach is to perform dynamic scaling analysis using power law model to

investigate strongly interacting nanoparticles. According to the power-law model for spin glass [108],

$$\tau = \tau_0 \left[\frac{T-T_g}{T_g}\right]^{-zv} \quad (7.4)$$

where T_g represents the glass transition temperature. The parameter *z* and *v* are dynamic exponent and spin- correlation length exponent, respectively. The parameter ν relates correlation length, ξ with reduced temperature by relation: $\xi \propto \left(\frac{T_p}{T_g} - 1\right)^{-v}$. The presence of equally relaxation time near glass temperature, T_g, suggests the existence of a finite temperature for equilibrium thermodynamic phase transition. A good fit for equation 4 was found with meaningful values for T_g= 184 ± 0.3 K, τ_0= 5 X $10^{-11\pm0.1}$ s and *zv* =11.8 as shown in figure 7.1(d) for ~2 nm silver shell. This value comes to be T_g= 171 ± 0.7 K, τ_0= 9 X $10^{-12\pm0.4}$ s and *zv* =12.7 as shown in figure 7.1(f) for 4 nm silver shell. The value obtained for T_g is smaller than T_b obtained from dc magnetization which is assumed to be due to the particle size distribution. The value of *zv* lies in the range between 4 and 12 for atomic spin glass compounds and moreover τ_0 is little slower than values for atomic spin-glass compounds [205], i.e. $\sim 10^{-12} - 10^{-14}\ s$. It is evident, from the result of the fits, that using power law model has a more physical significance than Neel- Arrhenius and Vogel-Fulcher model. The values obtained from power law model are very much closer and lies almost in range of spin glasses for this kind of system.

7.3 Magnetic Spin Dynamics in Electron-Rich Metal Coated on Magnetite Nanoparticles using Thermo-Remanent Magnetization Studies

The magnetization time decay measurements have been performed to confirm the spin glass behavior of samples under investigation. It is defined as measurement of time (*t*)

dependent magnetization on cooling a sample from well above freezing temperature (T_f) to the temperature of interest which is usually much lower than T_f, in presence of an

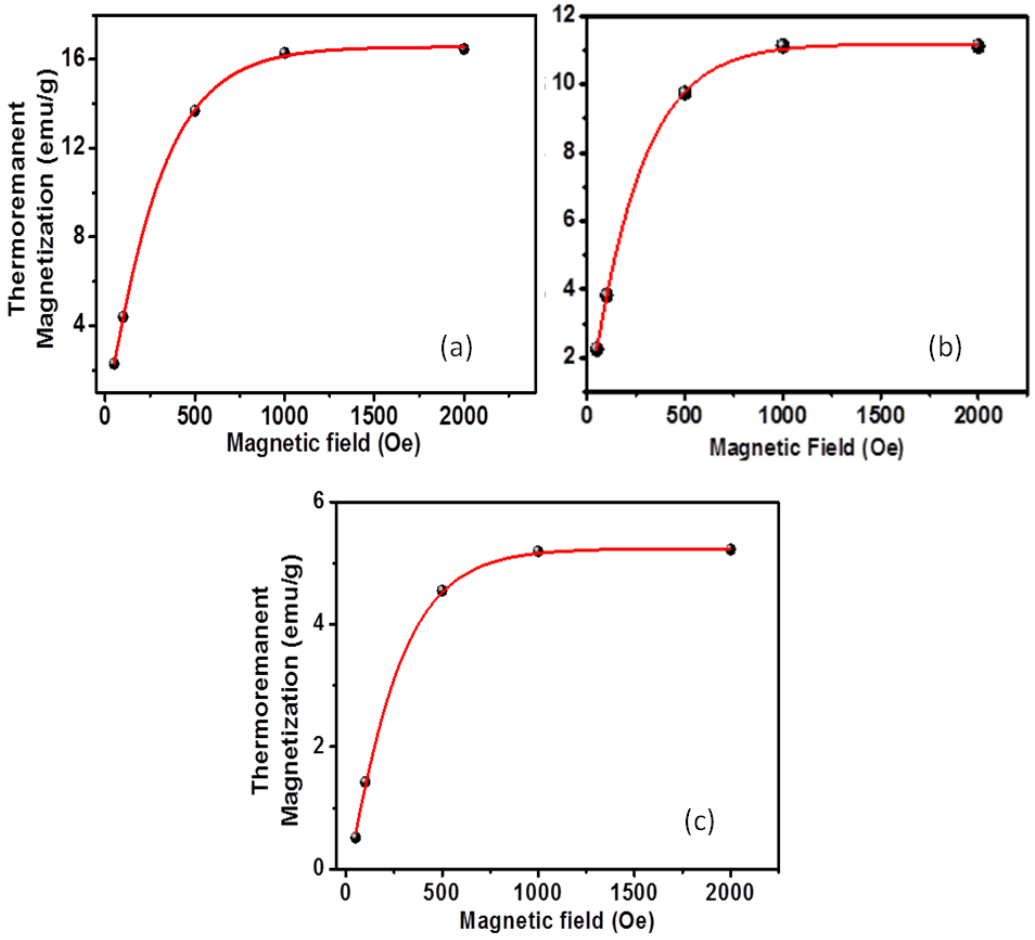

Figure 7.2 TRM plot against magnetic field for (a) uncoated magnetite nanoparticles, and (b) ~2 nm thick silver shell, and (c) ~4 nm thick silver shell coated magnetite nanoparticles.

applied field. The applied external field is then removed during the measurement of M *vs t*. In current work, to measure the magnetic relaxation and TRM values, we cool the sample in presence of 50 Oe magnetic field from temperature to 2 K from 300 K.

The TRM data of uncoated magnetite and silver coated magnetite nanoparticles were plotted against applied field that can be used to further distinguish between the magnetic

behaviors of different classes [206-207]. The value of magnetization (at t=0) corresponding to the applied field at specified temperature gives TRM value. For non-ergodic systems, the values of TRM should be non-zero. The TRM plot at 2 K (Figure 7.2 (a), (b) & (c)) show an increase in the values for smaller fields which is typical behavior of superparamagnetic or super spin glass systems in both the cases. A shallow decrease is observed in TRM value for 20 kOe, depicting the spin glass properties of the Fe_3O_4 and $Ag@Fe_3O_4$ core-shell nanoparticles. A similar type of behavior for TRM curve has been observed for maghemite nanoparticles which confirms our observation [202].

A spin glass system, on removal of externally applied field, relaxes very slowly to its minimum energy states. Most of the models show an exponential relaxing behavior for magnetization, i.e.$M\ (t) = M_0 exp\left(-\frac{t}{\tau}\right)$; τ being the time constant for an ideal case [104]. In case of real system, there is a distribution of relaxation times due to range of energy barriers. This distribution is incorporated in a stretched exponential function form given as [105]:

$$M(t) = M_0 - M_r \exp\left[-\left(\frac{t}{\tau}\right)^{1-n}\right] \tag{7.5}$$

to describe the magnetic relaxation in case of spin glasses. Here, M_0 and M_r relates to an intrinsic ferromagnetic and spin-glass components of observed relaxation effects, respectively. The M_r component contributes mainly to the observed relaxation effects. The value of M_r and τ are a function of temperature and waiting time after temperature stabilization, whereas n is only temperature dependent.

If there is a uniform distribution of energy barrier from zero to some constant high energy, the logarithmic decay of magnetization occurs according to equation [93]:

$$M(t) = M_0(t)\left[1 - S(T)\ln\frac{t}{\tau}\right] \tag{7.6}$$

where $S(T)$ is the magnetic viscosity defined as $S = \frac{1}{M_0}\frac{dM}{d(\ln t)}$.

If the magnetic relaxation time exhibits a critical slowing down, the power law form of magnetization decay $M(t) = M_0 t^{-n}$ is used where n is directly proportional to the temperature. In case of silver coated magnetite nanoparticles, it has been reported in our earlier studies, an intermediate disordered magnetic layer is formed in between magnetic core and non-magnetic shell. This leads to formation of a trilayer structure with three different magnetic characteristics arising from each layer is observed in a single nanoparticle. The innermost layer is composed of magnetite which ideally behaves like a superparamagnetic at room temperature for the particle size <20 nm. For lower temperature, the behavior exhibited is of generally ferrimagnetic/ ferromagnetic materials. The intermediate layer is considered to be magnetically disordered. The magnetic response or behavior of intermediate layer is quite unpredictable which needs to be investigated to predict its overall magnetic response. Thus, it can be said that the magnetic behavior shown by the system under study could be a combination of two same functions with different characteristic time or two different functions.

Figure 7.3 (a), 7.4 (a) and 7.5 (a) shows decay of magnetization with time in a log scale for uncoated, ~2 nm thick silver shell coated and ~4 nm thick silver shell coated magnetite nanoparticles, respectively. The slope of the line $S(t) = \frac{\partial M}{\partial \ln(t)}$ indicates the relaxation rate of the magnetic moments [93]. The two different values of $S(t)$ are clearly observable from the graph which points towards the existence of two characteristic relaxation time for the both set of nanoparticles under observation. The inflexion in slope occurs approximately at equal lapsed time whereas the slope difference increases sigmoidally with applied magnetic field.

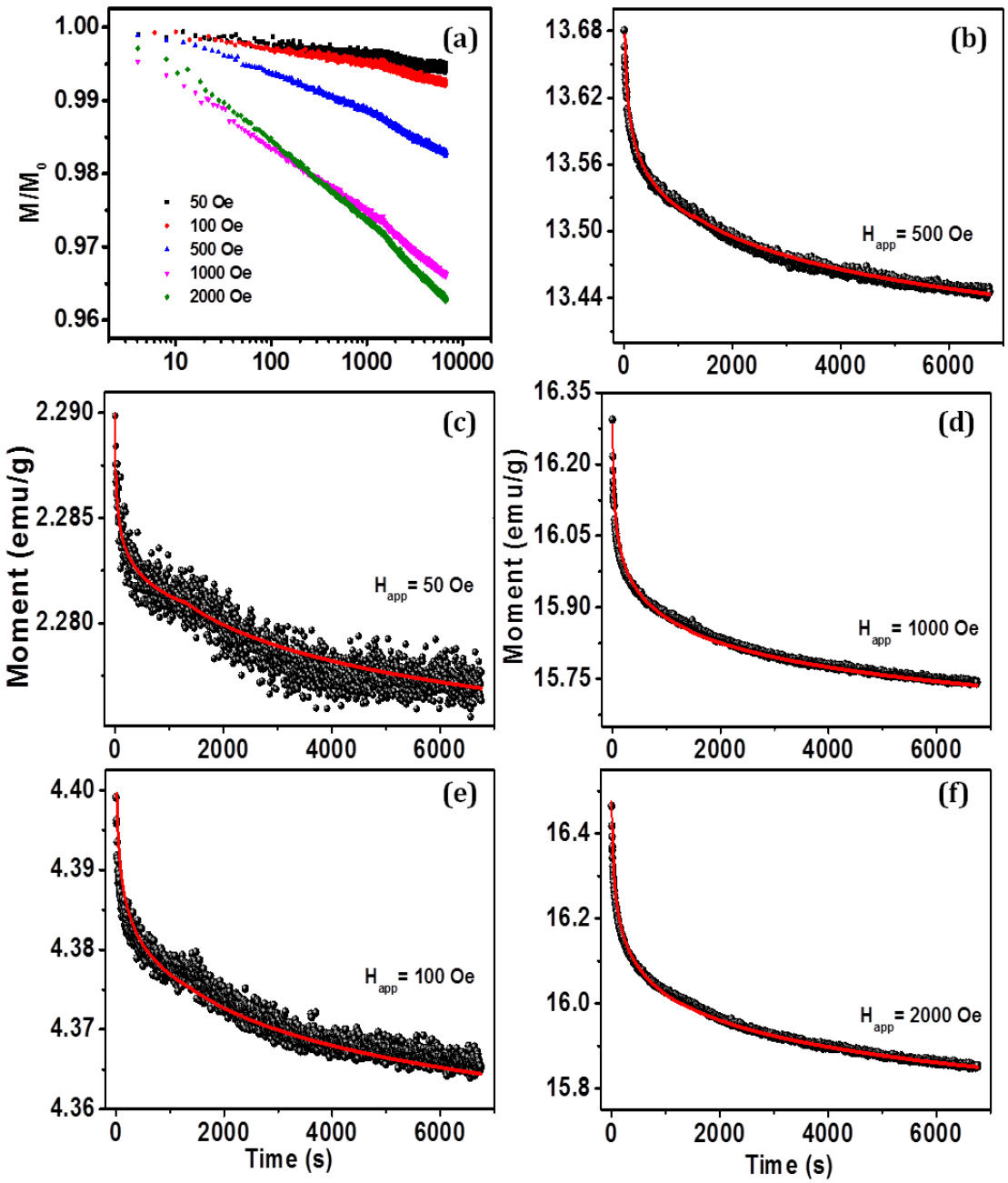

Figure 7.3 Magnetization time-decay plots for uncoated magnetite nanoparticles at temperature 2 K for different applied cooling fields (a) log scale variation of time for all fields (b) 50 Oe, (c) 100 Oe, (d) 500 Oe, (e) 1000 Oe and (f) 2000 Oe.

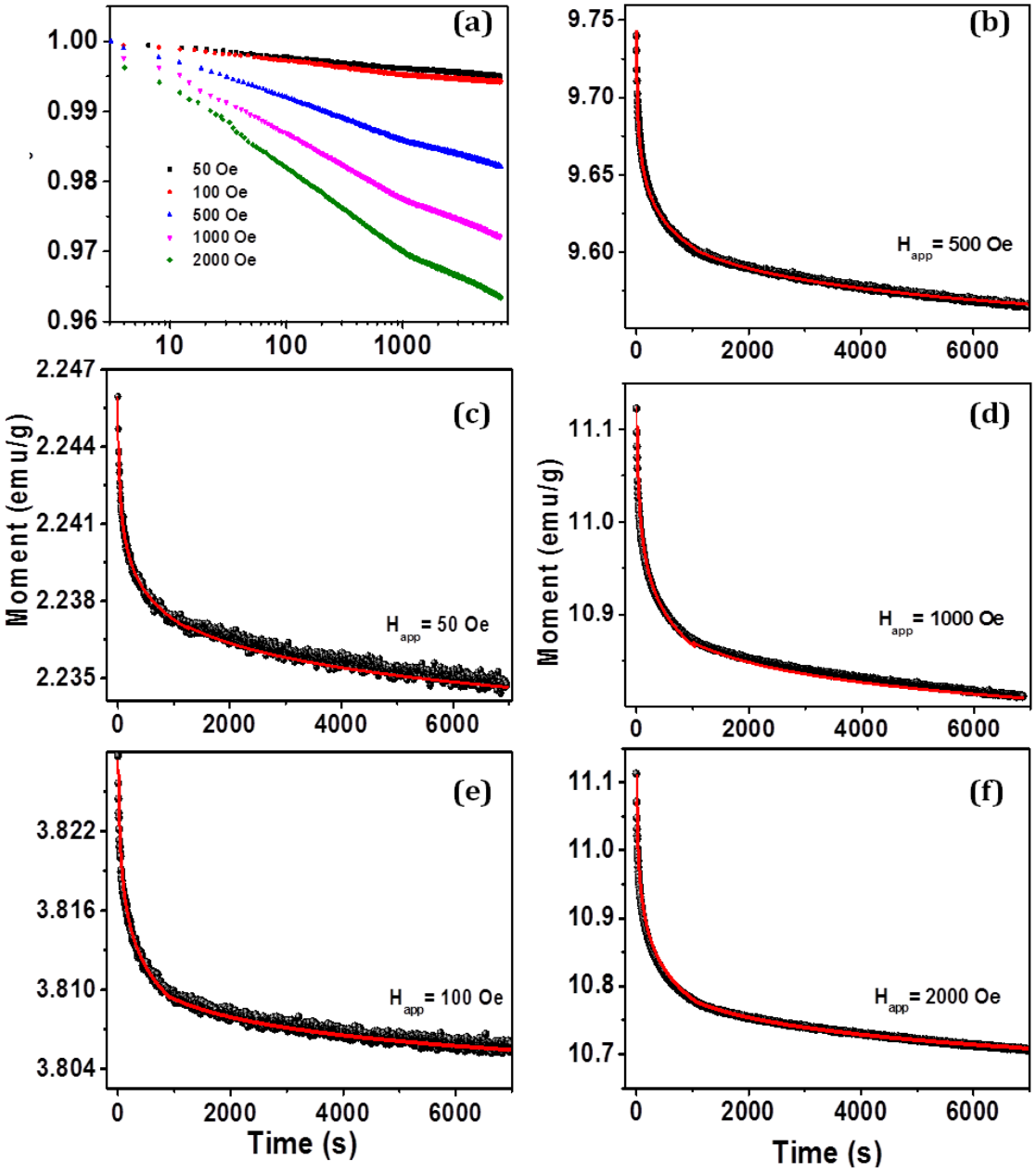

Figure 7.4 Magnetization time-decay plots for ~2 nm thick silver shell coated magnetite nanoparticles at temperature 2 K for different applied cooling fields (a) log scale variation of time for all fields (b) 50 Oe, (c) 100 Oe, (d) 500 Oe, (e) 1000 Oe and (f) 2000 Oe.

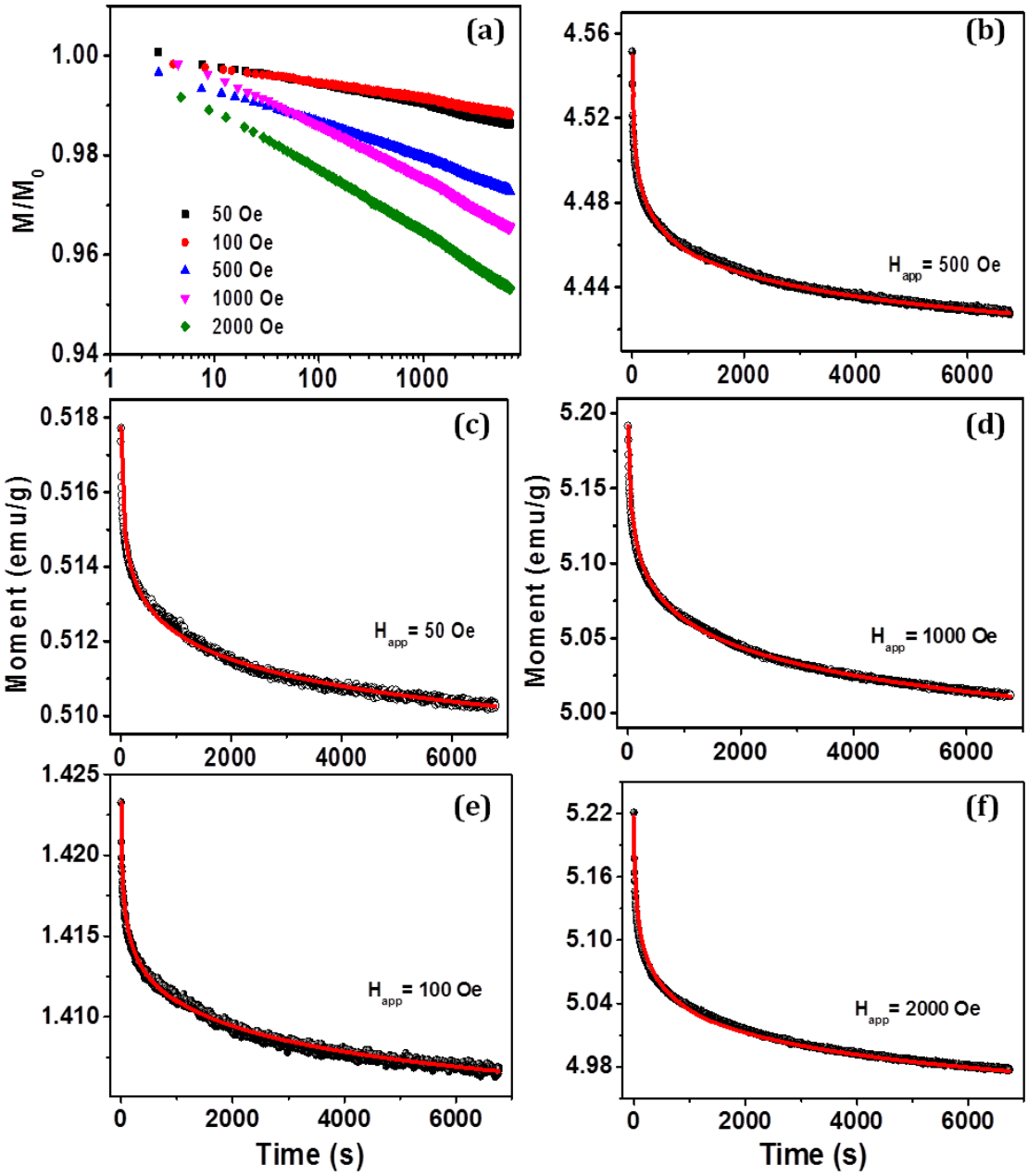

Figure 7.5 Magnetization time-decay plots for ~4 nm thick silver coated magnetite nanoparticles at temperature 2 K for different applied cooling fields (a) log scale variation of time for all fields (b) 50 Oe, (c) 100 Oe, (d) 500 Oe, (e) 1000 Oe and (f) 2000 Oe.

Amongst various relations and their combinations proposed to describe the magnetic relaxation, the two functional forms were found to be reasonably well- fitted [104-105],

$$M(t) = M_{01}(t)\exp\left(-\frac{t}{\tau_{11}}\right) + M_{02}(t)\exp\left(-\frac{t}{\tau_{12}}\right) \quad (7.7)$$

and, $$M(t) = M_0(t)\exp\left(-\frac{t}{\tau_{21}}\right) + M_0 - M_r \exp\left[-\left(\frac{t}{\tau_{22}}\right)^{1-n}\right] \quad (7.8)$$

The equation 7.7 is a combination of Neel-Arrhenius formalism with two distinct characteristic relaxation times of superparamagnetic spins in the trilayered structure, τ_{11} and τ_{12} while equation 7.8 is a combination of Neel-Arrhenius relaxation as well as stretched exponential form. In equation 7.8, τ_{21} and τ_{22} are the relaxation times for spins with superparamagnetic and spin-glass behavior, respectively. The value of M_r and τ_{22} is a function of time elapsed and temperature whereas n only depends on T. The value of n decides the presence of relaxation phenomena in spin glass. The value of n has been fixed as 0.92 for all the fittings as magnetization data has been recorded at a single temperature with different cooling fields. The solid lines in figure 7.3, 7.4 and 7.5 (b-e) represent best fits of equation 8 with our experimental data. The two different relaxation time τ_{21} and τ_{22} are obtained with considerable variation on application of varying magnitude cooling field. The τ_{21} value decreases from 1.73×10^{-12}s to 7.95×10^{-10}s and 1.69×10^{-13}s to 1×10^{-11}s for uncoated and ~2 nm thick silver coated nanoparticles, respectively, when cooling field magnitude is raised from 50 Oe to 2000 Oe. With same raise in cooling fields for ~4 nm thick silver shell coated magnetite nanoparticles, the value of $\tau_{21}$is obtained to be 3.7×10^{-15}s to 9.04×10^{-13} s. The values of τ_{22} show decrease from 21 s to 1×10^{-2} s, 4 s to 4×10^{-3} s and 0.39 s to 5.6×10^{-4} s for uncoated, ~2 nm thick silver shell and ~4 nm thick silver shell coated nanoparticles, respectively, in the described cooling field variation. The presence of thin

disordered spin layer at the nanoparticle surface is responsible for the contribution of spin-glass behavior in uncoated magnetite nanoparticles.

TABLE 7.1 Summary of fitting parameters obtained from fitting experimental TRM data for uncoated magnetite nanoparticles using combined functional forms. The value of n for SPM-SG combination has been fixed as 0.92.

S. No.	Applied Magnetic Field Intensity (in Oe)	T values from SPM-SPM combination (in s)		R^2 Values	T values from SPM-SG combination (in s)		R^2 Values
		τ_{11}	τ_{12}		τ_{21}	τ_{22}	
1	50	447(8)	4632(31)	0.9851	$1.73 \times 10^{-12\pm0.3}$	21(2)	0.9945
2	100	538(5)	4448(26)	09847	$1.34 \times 10^{-11\pm0.4}$	12(1)	0.9895
3	500	586(6)	4311(17)	0.9816	$9.21 \times 10^{-11\pm0.2}$	0.8(7)	0.9931
4	1000	610(5)	4193(12)	0.9871	$3.68 \times 10^{-10\pm0.5}$	0.4(3)	0.9873
5	2000	629(4)	4054(18)	0.9957	$7.95 \times 10^{-10\pm0.3}$	0.01(5)	0.9987

TABLE 7.2 Summary of fitting parameters obtained from fitting experimental TRM data for ~2 nm thick silver shell coated magnetite nanoparticles using combined functional forms. The value of n for SPM-SG combination has been fixed as 0.92.

S. No.	Applied Magnetic Field Intensity (in Oe)	T values from SPM-SPM combination (in s)		R^2 Values	T values from SPM-SG combination (in s)		R^2 Values
		τ_{11}	τ_{12}		τ_{21}	τ_{22}	
1	50	162(3)	3480(10)	0.9848	$1.69 \times 10^{-13\pm0.2}$	4(1)	0.9867
2	100	188(2)	3300(8)	09836	$9.39 \times 10^{-13\pm0.5}$	0.5(3)	0.9884
3	500	199(2)	3186(21)	0.9922	$1.34 \times 10^{-12\pm0.3}$	0.16(1)	0.9961
4	1000	220(3)	3124(11)	0.9901	$9.9 \times 10^{-12\pm0.2}$	0.034(2)	09966
5	2000	228(1)	3100(5)	0.9873	$1 \times 10^{-11\pm0.3}$	0.004(3)	0.9962

The thickness of this specific disordered spin layer gets enhanced on inclusion of the silver shell on the magnetite nanoparticles. The spin-glass relaxation becomes faster whereas relaxation with Neel-Arrhenius behavior shows a slower relaxation with increasing cooling fields. **Table 7.1**, **7.2** and **7.3** gives the value of τ_{11} and τ_{12} obtained by fitting experimental data with equation 7.7.

The values obtained using equation 7.8 has a more physical meaning than equation 7 in all three cases. The co-efficient of determination R^2 for the fit determines the quality of fit. The closer R^2 is to unity, the better is the fit. The comparison between R^2 values of both equations shows a much fitted value for equation8 that suggests the description of magnetic relaxation of both uncoated and trilayered core-shell nanoparticles is best defined by a combination of Vogel-Fulcher with a stretched exponential form. This finding indicates consolidated superparamagnetic and spin-glass magnetic behavior observed in a single nanostructure of uncoated and silver coated magnetite nanoparticles.

TABLE 7.3. Summary of fitting parameters obtained from fitting experimental TRM data for ~4 nm thick silver shell coated magnetite nanoparticles using combined functional forms. The value of n for SPM-SG combination has been fixed as 0.92.

S. No.	Applied Magnetic Field Intensity (in Oe)	T values from SPM-SPM combination (in s)		R^2 Values	T values from SPM-SG combination (in s)		R^2 Values
		τ_{11}	τ_{12}		τ_{21}	τ_{22}	
1	50	57(6)	2361(17)	0.9695	$3.7 \times 10^{-15\pm0.1}$	0.39(3)	0.9956
2	100	71(3)	2180(13)	09765	$8.79 \times 10^{-15\pm0.6}$	0.12(5)	0.9974
3	500	82(4)	1976(8)	0.9789	$2.01 \times 10^{-14\pm0.3}$	0.029(6)	0.9877
4	1000	89(2)	1850(10)	0.9732	$1.54 \times 10^{-13\pm0.2}$	0.008(7)	09894
5	2000	95(3)	1784(11)	0.9783	$9.04 \times 10^{-13\pm0.4}$	0.00056(4)	0.9981

7.4 Conclusions

In current chapter, we report the impact of silver coating over magnetite core nanoparticles on its magnetic relaxation behavior. The magnetite nanoparticle of size ~6.5 nm synthesized by microemulsion technique further coated by ~2 nm and ~4 nm thick silver shells were investigated. From ac susceptibility measurements, we calculated quantitative relative peak shift with respect to frequency, the value of which is an indicative of spin-glass behavior for silver coated magnetite nanoparticle which has been further verified using power-law model. The time-decay measurement of magnetization data, however, suggests presence of two different characteristic relaxation times in both uncoated and silver coated magnetite nanoparticles. On further comparison of experimental data with combination of magnetic relaxation functional forms, the Fe_3O_4 and Ag coated Fe_3O_4 nanoparticles were observed to have integrated magnetic behavior of superparamagnetic as well as spin glass systems.

After the determination of shape and size of these synthesized magnetite and silver coated magnetite nanoparticles, studying the time dependent and field dependent magnetization properties and the dynamics of magnetic spins, the investigation for their application in hyperthermia is discussed in the next chapter. The next chapter also presents the overall summary and future directions.